TISSUE ENGINEERING: Part A
Volume 19, Numbers 11 and 12, 2013

DOI: 10.1089/ten.tea.2012.0367

Human Perivascular Stem Cells Show Enhanced Osteogenesis and Vasculogenesis with Nel-Like Molecule I Protein

Asal Askarinam, BS,[1,*] Aaron W. James, MD,[1–3,*] Janette N. Zara, MD,[2] Raghav Goyal, BS,[1] Mirko Corselli, PhD,[2] Angel Pan,[1] Pei Liang, PhD,[2] Le Chang,[1] Todd Rackohn, BS,[1] David Stoker, MD,[4] Xinli Zhang, MD, PhD,[1] Kang Ting, DMD, DMedSc,[1,2] Bruno Péault, PhD,[2] and Chia Soo, MD, FACS[2]

An ideal mesenchymal stem cell (MSC) source for bone tissue engineering has yet to be identified. Such an MSC population would be easily harvested in abundance, with minimal morbidity and with high purity. Our laboratories have identified perivascular stem cells (PSCs) as a candidate cell source. PSCs are readily isolatable through fluorescent-activated cell sorting from adipose tissue and have been previously shown to be indistinguishable from MSCs in the phenotype and differentiation potential. PSCs consist of two distinct cell populations: (1) pericytes (CD146+, CD34−, and CD45−), which surround capillaries and microvessels, and (2) adventitial cells (CD146−, CD34+, and CD45−), found within the tunica adventitia of large arteries and veins. We previously demonstrated the osteogenic potential of pericytes by examining pericytes derived from the human fetal pancreas, and illustrated their *in vivo* trophic and angiogenic effects. In the present study, we used an intramuscular ectopic bone model to develop the translational potential of our original findings using PSCs (as a combination of pericytes and adventitial cells) from human white adipose tissue. We evaluated human PSC (hPSC)-mediated bone formation and vascularization *in vivo*. We also examined the effects of hPSCs when combined with the novel craniosynostosis-associated protein, Nel-like molecule I (NELL-1). Implants consisting of the demineralized bone matrix putty combined with NELL-1 (3 μg/μL), hPSC (2.5×10^5 cells), or hPSC+NELL-1, were inserted in the bicep femoris of SCID mice. Bone growth was evaluated using microcomputed tomography, histology, and immunohistochemistry over 4 weeks. Results demonstrated the osteogenic potential of hPSCs and the additive effect of hPSC+NELL-1 on bone formation and vasculogenesis. Comparable osteogenesis was observed with NELL-1 as compared to the more commonly used bone morphogenetic protein-2. Next, hPSCs induced greater implant vascularization than the unsorted stromal vascular fraction from patient-matched samples. Finally, we observed an additive effect on implant vascularization with hPSC+NELL-1 by histomorphometry and immunohistochemistry, accompanied by *in vitro* elaboration of vasculogenic growth factors. These findings hold significant implications for the cell/protein combination therapy hPSC+NELL-1 in the development of strategies for vascularized bone regeneration.

Introduction

Bone grafts are the current standard for treating non-healing skeletal defects.[1] However, the disadvantages associated with bone graft harvests are significant, including limited endogenous supply, prolonged surgical times, and harvest complications.[1–4] Cell sources such as bone marrow mesenchymal stem cells (BMSCs) and adipose-derived stem cells (ASCs) have generated significant interest for their tissue engineering potential.[5–7] However, the limitations associated with these conventional stem cell sources are also significant. BMSCs, for example, are difficult to harvest, are also in limited supply, and show reduced stem cell activity in aged and osteoporotic patients.[8,9] Further, BMSCs and ASCs

[1]Dental and Craniofacial Research Institute and Section of Orthodontics, School of Dentistry, UCLA, Los Angeles, California.
[2]UCLA and Orthopaedic Hospital Department of Orthopaedic Surgery and the Orthopaedic Hospital Research Center, University of California, Los Angeles, Los Angeles, California.
[3]Department of Pathology and Laboratory Medicine, David Geffen School of Medicine, University of California, Los Angeles, Los Angeles, California.
[4]Division of Plastic and Reconstructive Surgery, University of Southern California, Los Angeles, California.
*These two authors are co-first authors.

require *in vitro* expansion, which precludes the use of autologous cells in an emergency situation, and also introduces the risk of immunogenicity, infection, and genetic instability.[10] To avoid these shortcomings, studies have also investigated the use of an uncultured stromal vascular fraction (SVF) of adipose tissue. However, a side-by-side comparison reported lower bone formation among the uncultured SVF relative to cultured ASCs.[11] Moreover, SVF is a heterogeneous cell population that contains numerous nonstem cell types, such as inflammatory cells, hematopoietic cells, and endothelial cells, among others.[12–14] Heterogeneity complicates characterization of cell composition and introduces variability across samples. Such inconsistencies hamper efforts toward a reliable and standardized cell-based therapeutic for bone regeneration.

As an alternative stem cell source, our laboratories first identified and then prospectively isolated a perivascular mesenchymal stem cell (MSC)-like population. This MSC population, termed perivascular stem cells (PSCs), is found in all vascularized tissue[15,16] and consists of (1) CD146+ CD34− CD45− pericytes,[15,17] which line capillaries and microvessels, and (2) CD146− CD34+ CD45− adventitial cells,[18] found in the tunica adventitia of large arteries and veins. Pericytes were the first perivascular population studied, and were recognized for their expression of characteristic MSC markers (including CD10, CD13, CD44, CD73, CD90, and CD105).[15] The similarity of pericytes to MSCs was confirmed by demonstrating their ability to differentiate into multiple mesodermal lineages *in vitro*.[15] Clonal analysis of pericytes also showed expression of MSC markers and trilineage potential (differentiation into osteoblasts, chondrocytes, and adipocytes).[15] Likewise, subsequent studies demonstrated that adventitial cells, although located in a different location with respect to blood vessels, also expressed MSC markers and also displayed clonal multilineage potential in culture.[18] Further, pericytes and adventitial cells each comprise a significant portion of SVF of human adipose tissue (17.1% and 22.5%, respectively), with a combined average of 39.6%.[19] From a tissue engineering perspective, the isolation of the maximum MSC number per unit autologous tissue would be highly advantageous. To this end, in the present study, we combined the two PSC subpopulations (which constitute nearly 40% total SVF) and characterized their bone-forming potential. This approach maximizes the total number of MSCs collected per harvest, thus reducing the harvest morbidity.

There exist significant advantages to using fluorescence-activated cell sorting (FACS)-purified PSCs for tissue engineering purposes. First, purity ensures the specific and consistent use of only those cells known to participate in bone differentiation. This eliminates extraneous components of SVF, such as osteogenic differentiation-inhibiting endothelial cells, which may interfere with bone formation.[14] Recently, we reported that hPSCs form significantly more bone *in vivo* in comparison to an equal number of unpurified SVF cells of human adipose tissue.[19] To verify that this significant difference was due to the superior bone formation of purified hPSCs and not to a dilution effect resulting from the fewer number of MSCs found within the heterogeneous population of SVF cells, we also added the human SVF (hSVF) cells at a ratio of 10:1 to hPSCs in an intramuscular ectopic bone model. More bone was still observed with hPSC than with hSVF treatment, confirming the robust osteogenic potential of PSCs.[19] Further, in terms of a future cell-based therapeutic, a purified stem cell source also guarantees precise product characterization. This is important for any treatment seeking the Food and Drug Administration approval, as variability may raise concerns regarding consistency, safety, and efficacy. Finally, because PSCs are found in virtually all vascularized tissue, they are abundant and easily harvestable.[15] Given its superficial location and relative abundance, adipose tissue is an ideal tissue source for PSCs.

While purity, availability, and abundance make hPSCs an attractive stem cell source, their potential trophic effects on vascularization are also significant. Bone receives nutrients, oxygen, osteoinductive factors, and stem cells through the blood.[20] Therefore, an appropriate stem cell population for bone regeneration would also have proangiogenic effects.[20,21] Pericytes are known to maintain endothelial cell function,[22,23] and available studies have also shown that these cells secrete more angiogenic factors, such as vascular endothelial growth factor (VEGF) and fibroblast growth factor-2 (FGF-2), than do ASCs.[24,25] In our previous publication,[24] our laboratory examined pericytes derived from the human fetal pancreas, finding significant pro-osteogenic and provasculogenic effects. In the present study, we used an intramuscular ectopic bone model to develop the translational potential of our original findings now using PSCs from adult, human white adipose tissue. Therefore, our objectives were to (1) demonstrate the osteogenic and (2) vasculogenic potential of hPSCs (as a combination of pericytes and adventitial cells) and (3) pursue Nel-like Molecule I (NELL-1) as a growth factor capable of enhancing hPSC osteogenesis and vascularization.

Methods

Isolation of SVF from human lipoaspirate

Human lipoaspirate donated from $n=2$ healthy 31- and 40-year-old female patients was obtained after standard liposuction procedures. Lipoaspirate was collected from back, hip, flanks, and medial thigh. The hSVF was prepared by digesting the lipoaspirate with collagenase as previously described.[18] Briefly, the lipoaspirate was washed in an equal volume of phosphate-buffered saline (PBS) and centrifuged. The tissue layer was removed and mixed with a digestion solution (RPMI, 3.5% bovine serum albumin [BSA], 10 ng/mL DNAse, and 1 mg/mL Collagenase II) and incubated for 70 min at 37°C. The filtered solution was then centrifuged. The pellet was removed and washed twice in PBS 5 mM ethylenediaminetetraacetic acid (EDTA) before a red blood cell lysis buffer (155 mM NH_4Cl, 10 mM $KHCO_3$, and 0.1 mM EDTA) was added. After three additional PBS washes and centrifugations, trypan blue staining was used to count the number of viable hSVF cells. These hSVF cells were then either implanted or processed for hPSC purification. Cells isolated from different donors were not pooled, but rather used individually in the study.

Purification of PSCs from SVF

hPSCs were isolated from each donor's hSVF by FACS, per a previously published protocol.[18] A portion of the isolated hSVF was centrifuged, and the resulting pellet was

incubated with a solution of PBS, anti-CD146, fluorescein isothiocyanate (Abd Serotec; 1:100), anti-CD45 APC-cy7 (BD Bioscience; 1:100), and anti-CD34 APC (BD Bioscience; 1:100). After 15 min of incubation at 4°C and a wash in PBS, the pellet was suspended in RPMI (1 mL/10^6) and 4′,6-diamidino-2-phenylindole (DAPI, 1:1000; Invitrogen) to identify and then eliminate dead cells before cell sorting. The solution was then filtered using a 70-μM cell filter and then run on the FACSAria cell sorter to first selectively isolate and to then combine the pericytes (CD146+, CD34−, and CD45−), and adventitial cells (CD146−, CD34+, and CD45−) that make-up the population of PSCs. A portion of these cells was either immediately used *in vivo* or plated for *in vitro* studies. In select experiments, cells were labeled with a red fluorescent dye for cell-tracking purposes (PKH26 fluorescent cell linker; Sigma-Aldrich).

Cell culture

Cells were expanded in Dulbecco's modified Eagle's medium, 20% fetal bovine serum, and 1% penicillin/streptomycin. Osteogenic differentiation of cells followed a previously published protocol.[26,27] The medium was supplemented with 300–600 ng/mL of NELL-1, as previously described.[28] Osteogenic differentiation was assessed using alkaline phosphatase (ALP) and alizarin red (AR) staining at 5 and 10 days of osteogenic differentiation, respectively (with or without 300 ng/mL NELL-1). The representative 38.4× ALP and AR staining ($n=3$) images were semiquantitatively analyzed using the magic wand tool of Adobe Photoshop CS5. RNA isolation and quantitative real time–polymerase chain reaction (RT-PCR) for osteogenic genes were performed as previously described after 7 days osteogenic of differentiation with or without NELL-1 (300 ng/mL), including Osteopontin (*Opn*) and Osteocalcin (*Oc*).[24] Next, growth factor secretion was quantified using PSCs with or without NELL-1 (300–600 ng/mL). Briefly, the cells were seeded at 80% confluency in 1% serum conditions, after an attachment medium was supplemented with NELL-1, and supernatant was harvested after 48-h treatment. Enzyme-linked immunosorbent assays for VEGF and FGF-2 were performed per the manufacturer's instructions (Invitrogen; Cat No. KHG0111, HKG0021). The groups were initially unlabeled for photographic documentation and later revealed for quantification.

Implant preparation

Ovine demineralized bone matrix (DBX) putty was used (100 μL; Musculoskeletal Transplant Foundation) and combined with either 0 or 300 μg of NELL-1 lyophilized onto 15 mg β-tricalcium phosphate (TCP) particles to ensure prolonged NELL-1 release.[29] In selected experiments, 2.5×10^5 of either hPSCs or hSVF cells, suspended in 20 μL of PBS, were added. In addition, as a comparison group, select implants were treated with bone morphogenetic protein (BMP)-2 (3.75 μg) and was likewise lyophilized onto β-TCP. The components of the implant were mechanically mixed before use. A detailed summary of each of the implant constituents is presented in Supplementary Table S1 (Supplementary Data are available online at www.liebertpub.com/tea). The DBX/β-TCP implant was chosen, as it is moldable putty with osteoinductive properties and reliable protein release kinetics, making it readily translatable to bone-defect models.

Surgical procedures

Eight-week-old male SCID mice were anesthetized by isoflurane inhalation (5% induction; 2% maintenance) and medicated with 0.05 mg/kg buprenorphine. As previously shown, bilateral incisions were made in the hind limbs, and pockets were created in the biceps femoris along the long axis of the muscle fiber, so that one implant may be inserted in each limb with ease and without lying in contiguity with the femoral bone (so as to not induce an osteoblastic response in the host femoral periosteum).[30] 5-0 Vicryl sutures were used to suture the overlying fasciae and skin. Postoperative care included buprenorphine for 48 h to manage pain and trimethoprim/sulfamethoxazole for 10 days to prevent infection. All surgical procedures were consistent with the regulations put forth by the UCLA Chancellor's Animal Research Committee.

Radiographic analysis

Muscle pouch samples were harvested 4 weeks after surgery, fixed in formalin, and imaged using high-resolution microcomputed tomography (microCT, Skyscan 1172F; Skyscan). Images were analyzed in CTAn to determine the bone volume ($n=8$) and bone mineral density (BMD, $n=8$). Specific threshold values are included in figure legends.

Histology and immunohistochemistry analysis

Samples were decalcified in 19% EDTA, embedded in paraffin, sectioned, and stained with hematoxylin and eosin (H&E). the representative 200× H&E images were semiquantitatively analyzed using the magic wand tool in Adobe Photoshop to evaluate the level of osteogenesis by such parameters as percent bone area (% B. Ar., $n=10$), relative bone area ($n=10$), osteocyte lacunar density ($n=15$), and percentage of filled lacunae ($n=15$).[31] Immunohistochemistry was performed for BMP-2 (Santa Cruz Biotechnology, Inc.), bone morphogenetic protein 7 (BMP-7; Santa Cruz Biotechnology, Inc.), Osteocalcin (OCN; Santa Cruz Biotechnology, Inc.), VEGF (Santa Cruz Biotechnology), von Willebrand Factor (vWF; US Biological), human β-2 microglobulin (Abcam), and proliferating cell nuclear antigen (PCNA; Dako). For immunohistochemistry, staining without a primary antibody was performed as a negative control throughout. Briefly, the paraffin slices were deparaffinized, dehydrated, rinsed, and incubated with 3% H_2O_2 for 20 min and then blocked with 0.1% BSA in PBS for 1 h. Primary antibodies at a dilution of 1:100 were added to each section and incubated at 37°C for 1 h and at 4°C overnight. The ABC complex (Vector Laboratories) was applied to the sections after the incubation with a biotinylated secondary antibody (Dako Corporation). 3-Amino-9-ethylcarbazole plus substrate in red color (Dako) was used as a chromagen, and the sections were counterstained with light hematoxylin. Immunofluorescent staining was performed on frozen sections for CD31 (Santa Cruz) and PCNA (Dako), using Alexa-488 streptavidin as a secondary antibody and a Hoechst 33324 counterstain (Sigma-Aldrich). The respective 400× images (OCN, n = 5; BMP-2, n = 8; BMP-7, n = 8; PCNA, n = 10) were analyzed by histomorphometric semiquantitative analysis using the magic wand tool in Adobe Photoshop to quantify the relative stain intensity across groups. To eliminate bias, slides were initially unlabeled for photographic documentation and later

revealed for quantification. Specific tolerance levels for Photoshop quantification are listed in the figure legends.

Statistics

A one-way analysis of variance was used when more than two groups compared. This was followed by a *post hoc* Tukey test to specifically compare the difference between two specific groups (as in Figs. 1J, K, 2B, 3B–E, 4D–F, and 6B–D). In addition, a Student *t*-test was used to test significance when only two groups were tested (as in Figs. 1F–I and 5C–E; Supplementary Fig. S1C). *p values ≤ 0.05 were significant.

Results

Isolation and in vitro *differentiation of hPSC*

FACS was used to isolate hPSCs from the SVF of adipose tissue according to our previously published protocol.[18] This MSC population consists of pericytes (CD146+, CD34−, and CD45−)[15] and adventitial cells (CD146−, CD34+, and CD45−).[18] After exclusion of DAPI+ dead cells and CD45+ hematopoietic cells (Fig. 1A, B), adventitial cells and pericytes were detected based on the differential expression of CD34 and CD146. CD34+CD146− adventitial cells and CD146+CD34− pericytes were then collected together as hPSCs for further *in vitro* and *in vivo* studies.

First, we evaluated hPSCs for *in vitro* osteogenic differentiation. hPSCs showed robust ALP staining after 5 days in an osteogenic differentiation medium (Fig. 1D) and robust AR staining at 10 days of osteogenic differentiation (Fig. 1E). Consistent with published reports in other cell types,[28,32] hPSCs treated with NELL-1 protein (300 ng/mL) showed an increase in both ALP and AR staining at 5 and 10 days of osteogenic differentiation, respectively (Fig. 1D, E). Semiquantitative analysis of the representative images confirmed a significant increase in ALP and AR staining when hPSCs were treated with NELL-1 (Fig. 1F, G). Next, osteogenic gene expression was evaluated in hPSCs, with or without NELL-1 treatment for 7 days of differentiation, including Osteopontin (*Opn*) and Osteocalcin (*Oc*) (Fig. 1H, I). NELL-1 resulted in an ~62–88% increase in *Opn* and *Oc* expression, respectively. Finally, we have previously shown that NELL-1 induces *Vegf* expression in human pericytes.[24] We sought to examine whether NELL-1 could likewise induce secretion of vasculogenic growth factors in hPSCs, including VEGF and FGF (FGF-2) (Fig. 1J, K). Results showed a striking dose-dependent increase in VEGF protein secretion in hPSCs with NELL-1 treatment (Fig. 1J). Likewise, NELL-1 induced FGF-2 protein secretion in hPSC across concentrations examined (300–600 ng/mL, Fig. 1K). These data demonstrate the osteogenic potential of hPSCs *in vitro* and the ability of NELL-1 to promote hPSC osteogenic differentiation and trophic factor production.

hPSCs form significantly more bone in vivo *when combined with NELL-1*

Next, an intramuscular ectopic bone model was used to evaluate the *in vivo* osteogenic potential of hPSCs in combination with NELL-1. DBX Putty® was selected as the osteoinductive carrier. Implants consisted of DBX alone or DBX with hPSCs, NELL-1 protein, or hPSCs+NELL-1 in combination. In addition, a BMP-2 comparison group was used (hPSCs+BMP-2). Implants were inserted intramuscularly in SCID mice to assess ectopic bone formation (see Supplementary Table S1 for treatment group specifics). Mice were harvested 4 weeks after surgery for evaluation of bone growth. Three-dimensional microCT showed an increase in bone formation in NELL-1-treated and PSC-treated samples (Fig. 2A). Notably, the combined hPSCs+NELL-1 treatment showed more bone formation than either cell or cytokine treatment alone. This trend was reflected in the microCT quantification of BMD (Fig. 2B). NELL-1 was also compared to the more commonly studied cytokine BMP-2. Results showed that BMP-2 induced significant ossification among PSC-treated samples, and induced a significantly higher BMD as compared to other treatment groups.

After microCT imaging and analysis, samples were evaluated histologically by routine H&E staining. Representative images of H&E-stained slides for hPSC-treated samples showed larger bone chips and reduced spacing between bone chips, as compared with the DBX control samples (Fig. 3A). These qualities were more apparent in samples with combined hPSCs and NELL-1 treatment, suggesting an additive effect of hPSC and NELL-1 on ectopic bone formation (Fig. 3A). In addition, hPSC+NELL-1-treated samples also showed evidence of endochondral ossification (see black arrow, Fig. 3A). In comparison, hPSC+BMP-2-treated samples showed robust new bone formation, but the spaces between bone chips were filled with notable lipid accumulation (see asterisks, Fig. 3A).

These H&E observations were next semiquantitatively confirmed with histomorphometric analysis of serial sections. Histomorphometric quantification of bone area (Fig. 3B) and % B. Ar. (Fig. 3C) per random high-powered field confirmed our initial observations. Both hPSC-treated samples and NELL-1-treated samples were observed to have significantly more bone than the DBX control, whereas samples treated with the combination hPSCs+NELL-1 showed significantly more bone than those treated with either cells or protein alone (Fig. 3B, C). This finding demonstrated the osteoinductive property of NELL-1, especially when combined with hPSCs. Notably, the bone area in the hPSC+NELL-1 samples was observed to rival that of hPSC+BMP-2 samples. Next, the osteocyte lacunar density was assessed, which measures the number of osteocytes per unit of bone area.[33] In this situation, the osteocyte lacunar density indicated both new bone formation and/or repopulation of the DBX particle lacunae. To calculate the osteocyte lacunar density, random high-powered images of H&E-stained slides for each group were used to determine the number of osteocytes per mm^2 of bone area. Again, a significant additive effect was observed with combined hPSC and NELL-1 treatment (Fig. 3D). Further, the percentage of filled lacunae was calculated to determine the percentage of DBX particle lacunae filled with osteocytes. Again, the combined hPSC and NELL-1 treatment had a significant additive effect (Fig. 3E). In summary, these data suggested that NELL-1 had a positive effect on hPSC osteoblastogenesis.

Immunohistochemical analysis of ectopic bone formation

Immunohistochemistry was next performed on the same experimental samples as in Figures 2 and 3. Specific stains included the bone matrix protein, OCN (Fig. 4A), and the bone cytokines of BMP-2 (Fig. 4B) and BMP-7 (Fig. 4C). OCN staining across all groups was located primarily within DBX

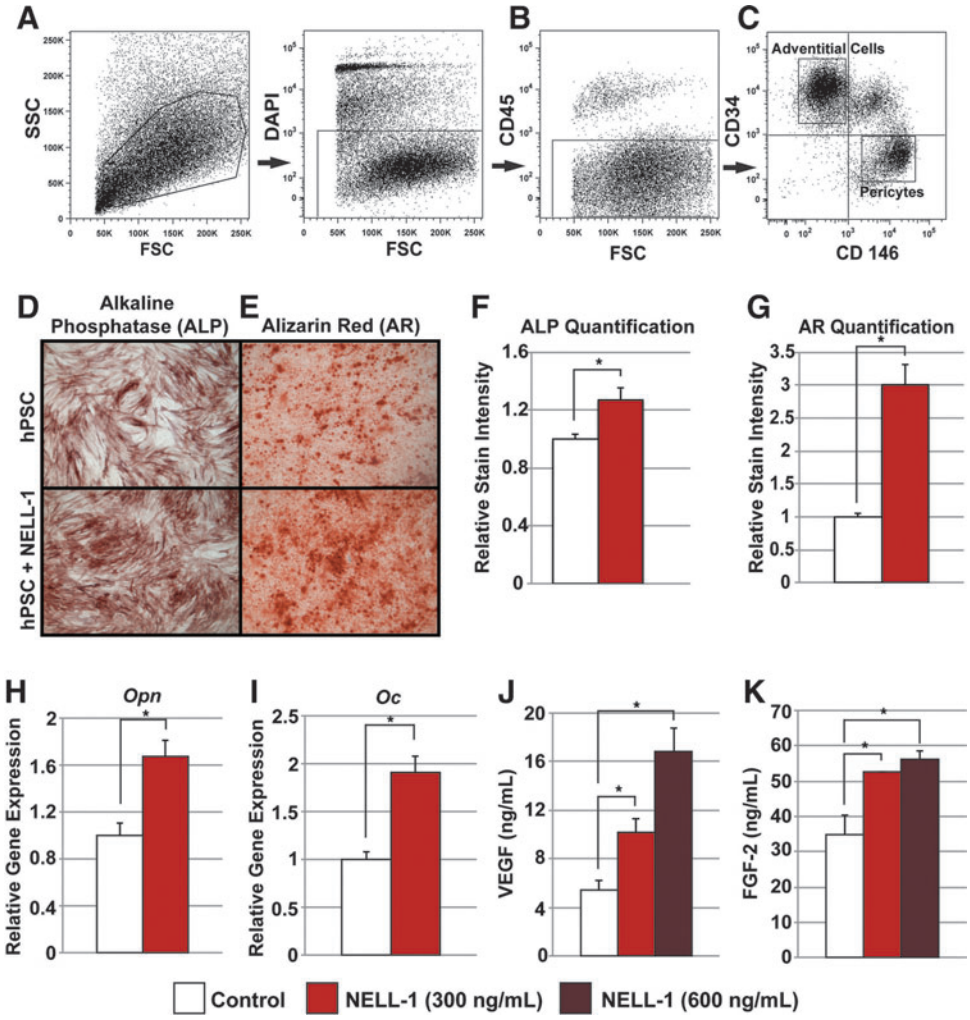

FIG. 1. Human perivascular stem cell (hPSC) isolation and *in vitro* osteogenic differentiation. **(A–C)** Fluorescence-activated cell sorting (FACS) isolation method for hPSCs. **(A)** 4′,6-Diamidino-2-phenylindole (DAPI)+ dead cells and **(B)** CD45+ hematopoietic cells were excluded before hPSC isolation. **(C)** Purified hPSCs consist of distinct CD34− and CD146+ pericytes and CD34+ and CD146− adventitial cells. **(D–G)** hPSCs were cultured under osteogenic conditions, treated with or without 300 ng/mL Nel-like Molecule I (NELL-1) protein. **(D)** Alkaline phosphatase (ALP) staining at 5 days of osteogenic differentiation. **(E)** Alizarin Red (AR) staining at 10 days of osteogenic differentiation. **(F)** Photographic semiquantitative analysis of ALP staining and **(G)** AR staining based on random $n=3$ (38.4×) images, using the Adobe Photoshop magic wand tool (tolerance of 32). **(H)** Osteopontin (*Opn*) expression by quantitative real time (RT)–polymerase chain reaction (qRT-PCR) at 7 days of differentiation. **(I)** Osteocalcin (*Oc*) expression by qRT-PCR at 7 days of differentiation. **(J)** Secreted vascular endothelial growth factor (VEGF) protein in the supernatant as assessed by enzyme-linked immunosorbent assay (ELISA) at 48-h treatment with NELL-1 (300–600 ng/mL). **(K)** Secreted FGF-2 protein in the supernatant as assessed by ELISA at 48-h treatment with NELL-1 (300–600 ng/mL). $^*p<0.05$. Color images available online at www.liebertpub.com/tea

chips and the newly formed bone. The hPSC-treated groups showed greater staining relative to the NELL-1-treated groups, while the combination hPSC and NELL-1-treatment showed the highest staining intensity (Fig. 4A). This observation was confirmed by a semiquantitative assessment by three blinded reviewers using Adobe Photoshop (Fig. 4D). Next, BMP-2 immunohistochemistry and semiquantification were performed (Fig. 4B, E). Across all samples, BMP-2 staining was primarily observed among the cells surrounding bone particles. As with OCN, the combined treatment of hPSCs and NELL-1 resulted in significantly higher staining of BMP-2 than either cells or cytokine alone. Finally, BMP-7 immunohistochemistry and quantification were performed (Fig. 4C, F). A similar overall distribution of BMP-7 was noted in comparison to BMP-2. Again, the hPSC and NELL-1 combination treatment induced significantly higher expression of BMP-7 when compared to either cell or cytokine treatment alone. Thus, the immunohistochemistry for the bone matrix protein OCN and bone cytokines, BMP-2 and BMP-7, revealed an additive effect of hPSCs and NELL-1 on the markers of bone formation.

Persistence and proliferation of hPSCs

To confirm that those cells within the implant site were in fact the implanted human cells, immunohistochemistry was performed for human β-2 microglobulin and PCNA. Both hPSC-treated and hPSC+NELL-1-treated samples showed

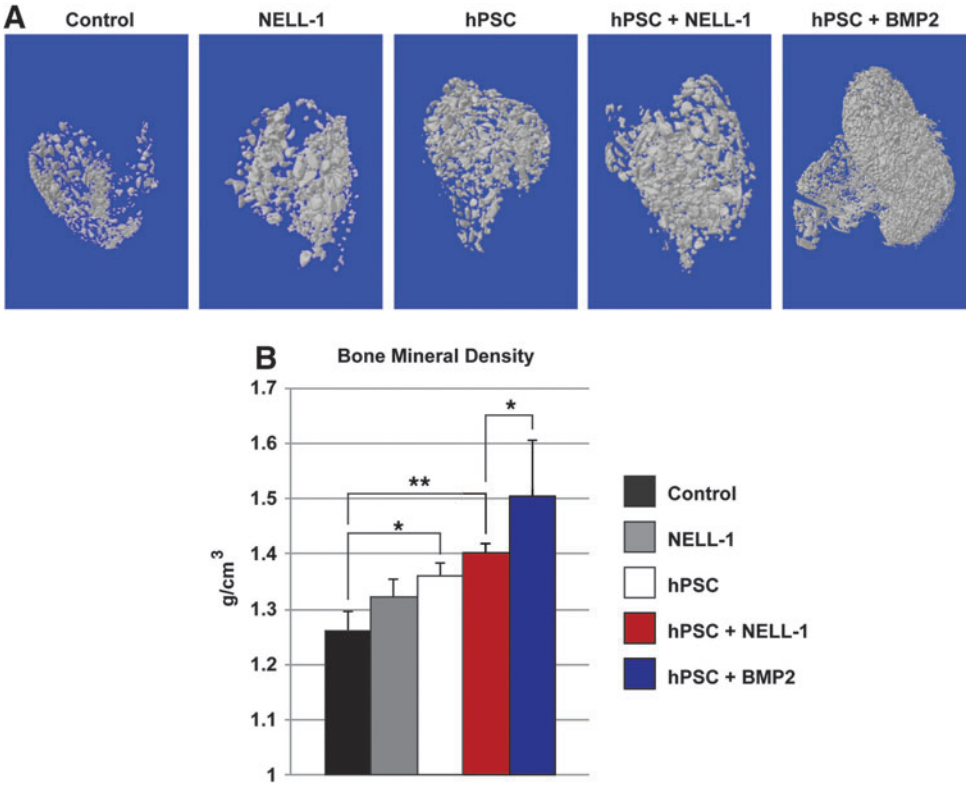

FIG. 2. hPSCs form significantly more bone *in vivo* when combined with NELL-1. Implants consisting of the demineralized bone matrix (DBX) or DBX treated with hPSCs (2.5×10^5 cells), NELL-1 (3 μg/μL), or both hPSC and NELL-1 were inserted intramuscularly in SCID mice. Bone morphogenetic protein-2 (BMP-2) protein was used as a comparison to NELL-1 (see Supplementary Table S1 for treatment group specifics). Mice were harvested 4 weeks post-implantation and evaluated for bone formation. **(A)** Representative three-dimensional microcomputed tomography images at Th120, and corresponding analysis of **(B)** mean bone mineral density (BMD, $n = 8$) (Th50–120 used for analysis). $^*p < 0.05$; $^{**}p < 0.01$. Color images available online at www.liebertpub.com/tea

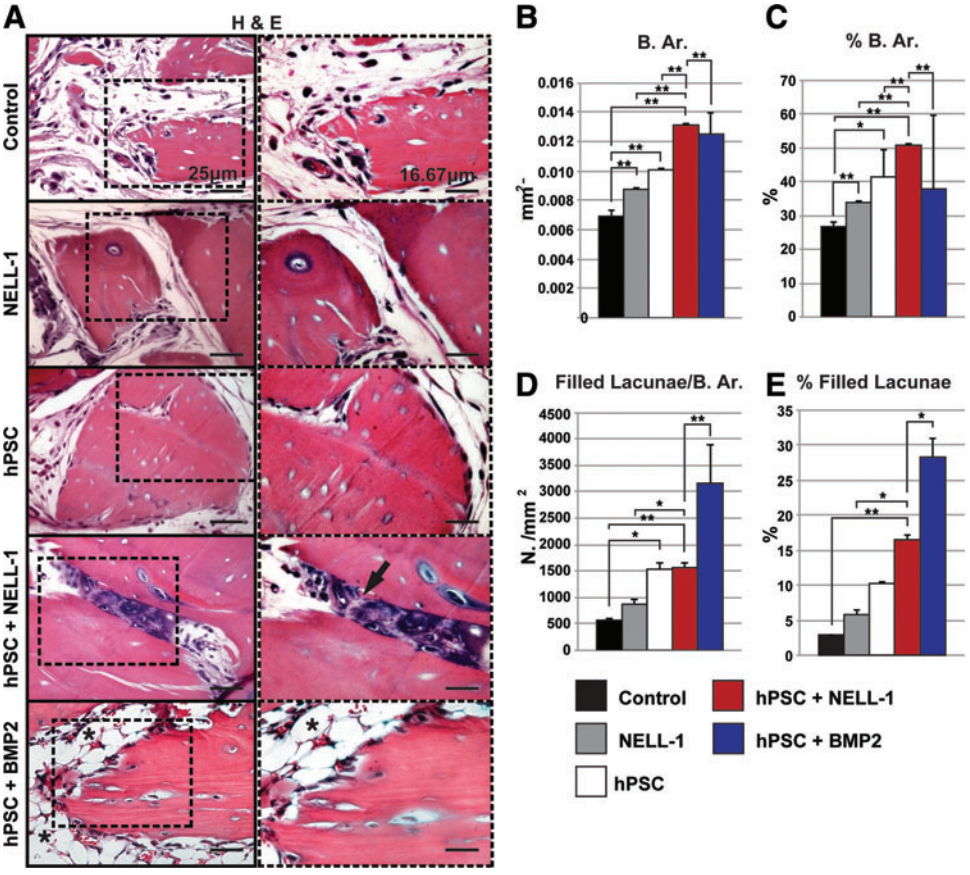

FIG. 3. Histological evidence of enhanced osteogenic potential of combined hPSC-NELL-1-treatment. Hematoxylin and eosin (H&E) staining was performed on the five previously mentioned experimental groups (DBX, DBX + NELL-1, DBX + hPSC, DBX + hPSC + NELL-1, and DBX + hPSC + BMP2). **(A)** Representative H&E images. **(B–E)** Histomorphometric semiquantitative analysis of random 200× H&E images: **(B)** Bone area (B. Ar), $n = 10$ images per group, tolerance = 50, **(C)** percent bone area (% B. Ar.), $n = 10$ images per group, tolerance = 50, **(D)** number osteocyte/bone area, (N. Oc/B. Ar.), $n = 15$ images per group, tolerance = 20, and **(E)** % filled lacunae, $n = 15$ images per group, tolerance = 20. $^*p < 0.05$; $^{**}p < 0.01$. Black arrow indicates endochondral ossification. Black asterisk indicated lipid accumulation. Color images available online at www.liebertpub.com/tea

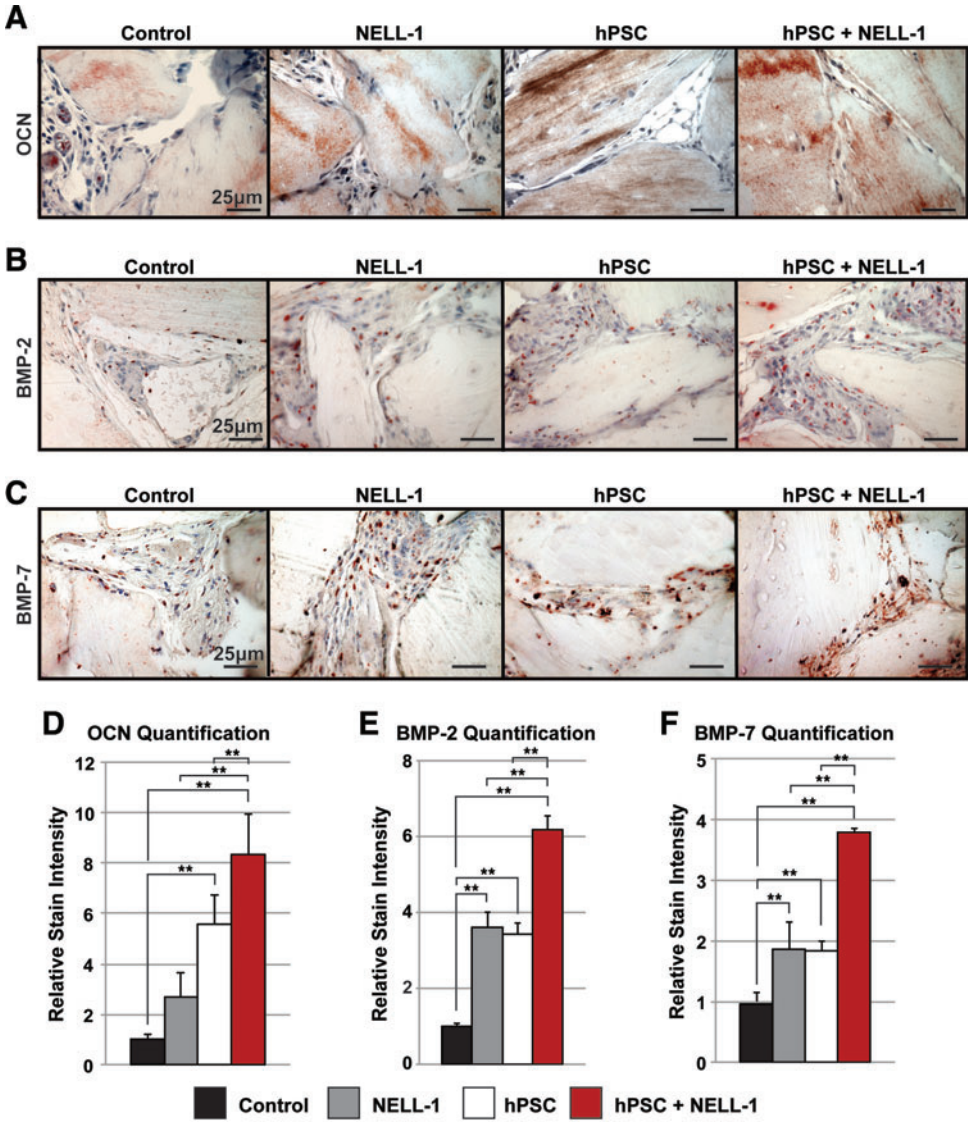

FIG. 4. Immunohistochemical analysis of ectopic bone formation. **(A–C)** Immunohistochemistry was performed on the four previously mentioned experimental groups (DBX, DBX + NELL-1, DBX + hPSC, and DBX + hPSC + NELL-1). Semiquantitative analysis of the relative stain intensity was determined, using the magic wand tool of Adobe Photoshop on random 400× fields. **(A)** Representative images of Osteocalcin (OCN) immunohistochemistry and corresponding relative stain quantification **(D)**, based on $n = 5$ images per group and tolerance of 30. **(B)** Representative images of BMP-2 immunohistochemistry and corresponding relative stain quantification **(E)**, based on $n = 8$ images per group and tolerance of 30. **(C)** Representative images of bone morphogenetic protein-7 (BMP-7) immunohistochemistry and corresponding relative stain quantification **(F)**, based on $n = 8$ images per group and tolerance of 30. $^{**}p < 0.01$. Color images available online at www.liebertpub.com/tea

distinct β-2 microglobulin staining between DBX chips at 4 weeks postimplantation, indicating the persistence of human cells (Supplementary Fig. S1A). In addition, PCNA immunostaining showed active cell proliferation within the implant site (Supplementary Fig. S1B). Moreover, semiquantification of PCNA staining using Adobe Photoshop showed a significant increase in the samples treated with hPSC + NELL-1, in comparison to hPSCs alone (Supplementary Fig. S1C). To test whether the PCNA + cells were of human (PSC) or mouse (host) origin, we next performed immunofluorescent staining (Supplementary Fig. S1D). Here, PCNA + cells appear green, while implanted cells were prelabeled with a red fluorochrome. A significant number of PCNA + cells were found to be implanted cells. Overall, this reflects the proliferative effect of NELL-1 on PSCs, in agreement with previous reports by our research group.[24]

hPSC-treated implants show an increase in vascularization

As mentioned, new bone formation and neovascularization are intimately connected. We next turned our attention to the effects of hPSC on blood vessel formation. For this comparison, an equal number of patient-matched unsorted hSVF cells or purified hPSCs were implanted. To visualize and quantify the size and number of blood vessels, the slides were first stained with H&E. Representative H&E images of hSVF-treated and hPSC-treated samples showed a notable difference in the size and number of blood vessels (Fig. 5A, B). Semiquantitative histomorphometric analysis of H&E-stained images showed a significant increase in both the blood vessel size (Fig. 5C) and number (Fig. 5D) in hPSC-treated samples. To further confirm these differences, immunohistochemistry was performed for VEGF. VEGF is a major angiogenic factor that promotes vascularization by regulating endothelial cell proliferation and migration.[20] Samples treated with hPSCs showed greater VEGF staining in comparison to those treated with hSVF (Fig. 5A, B). This was quantified, showing a significant increase in VEGF expression in the hPSC-treated samples in comparison to hSVF (Fig. 5E). Next, the hSVF-treated and hPSC-treated implants were examined for vWF immunohistochemistry. Representative images showed greater vWF staining in the hPSC-treated samples than in the hSVF-treated samples (Fig.

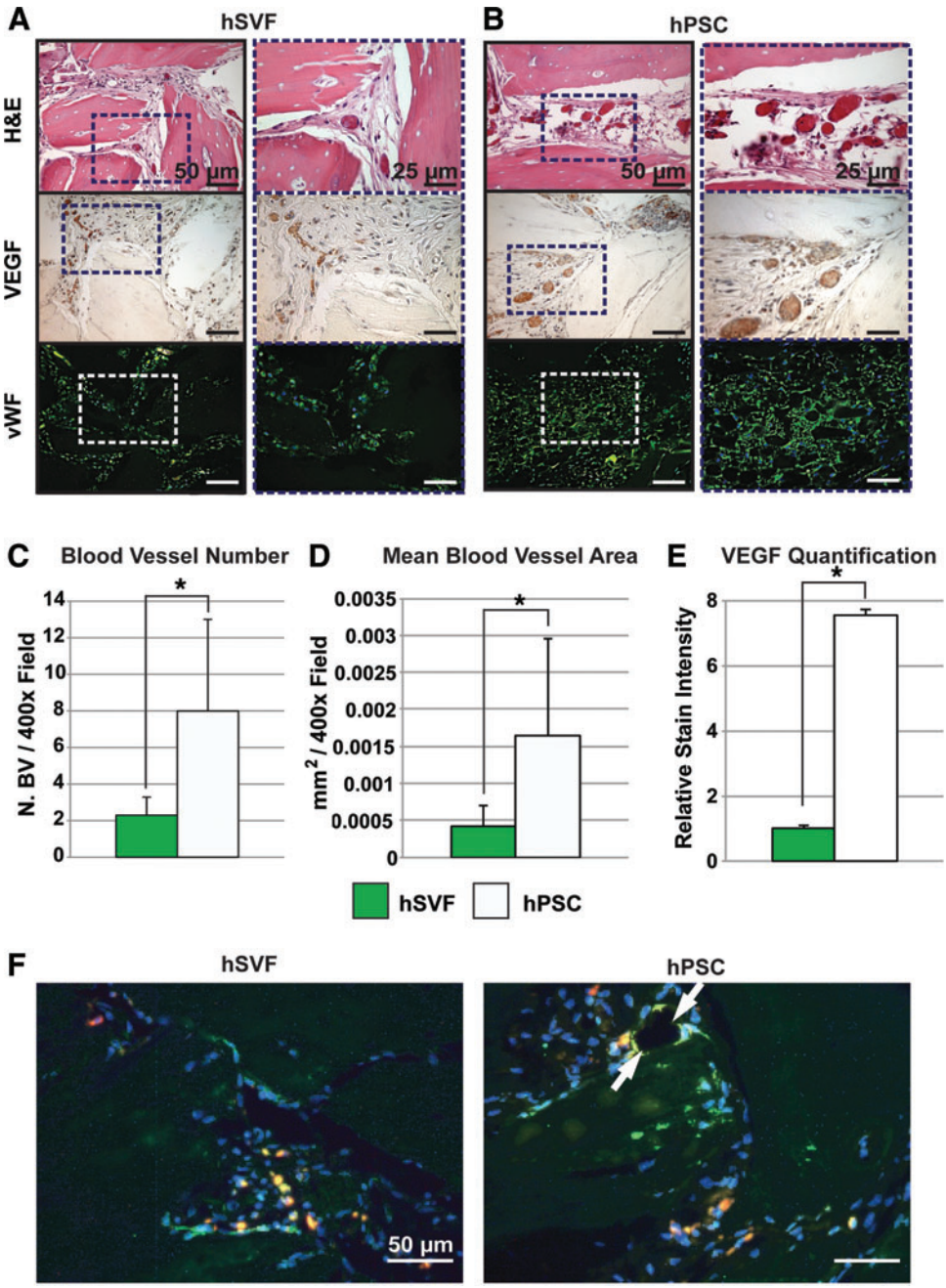

FIG. 5. hPSC-treated implants show increased vascularization as compared to the human stromal vascular fraction (hSVF). Equal numbers (2.5×10^5) of either hPSCs or hSVF cells loaded onto DBX putty were implanted intramuscularly. Samples were harvested 4 weeks postimplantation. Specimens were stained with H&E and for VEGF and von Willebrand Factor (vWF). Histomorphometric semiquantitative analysis of respective 400× images followed using the Adobe Photoshop magic wand tool. **(A)** H&E, VEGF, and vWF staining among hSVF-treated implants. **(B)** H&E, VEGF, and vWF staining among hPSC-treated implants. **(C)** Blood vessel number, based on $n = 10$ H&E images per group. **(D)** Mean blood vessel area, based on $n = 10$ H&E images per group at a tolerance of 30. (**E**) VEGF quantification, based on $n = 5$ images per group and tolerance of 30. **(F)** CD31 immunofluorescent staining, appearing green with red fluorescent-labeled cells. DAPI is used as a nuclear counterstain, appearing blue. White arrow indicates close association of PSCs with a blood vessel. $^*p < 0.05$. Color images available online at www.liebertpub.com/tea

5A). Finally, CD31 immunofluorescent staining (a marker of endothelial cells) was performed in samples implanted with red fluorescent-tagged cells (Fig. 5F). We found that red-labeled PSCs frequently were found in a close association with CD31+ endothelial cells within the vasculature. In contrast, the red-labeled SVF cells showed are more sporadic and less close association with blood vessels. These studies collectively confirmed the significantly larger effect that hPSCs have on vascularization in comparison to unsorted hSVF.

NELL-1 enhances the hPSC-mediated effect on vascularization

Finally, the effect of NELL-1 on hPSC-mediated vascularization was examined. NELL-1 has previously been reported to have proangiogenic effects.[24] We returned to the intramuscular samples from Figures 2 and 3, examining the effects of NELL-1 on hPSC-mediated vascularization. Samples were first stained with H&E (Fig. 6A). H&E-stained images and corresponding semiquantitative histomorphometric analysis revealed an increase in the blood vessel number (Fig. 6B) and size (Fig. 6C) in the NELL-1-treated and hPSC-treated samples relative to the DBX control. The hPSC + NELL-1-treated samples showed the highest blood vessel number and greatest blood vessel size relative to either cell or cytokine treatment alone. This finding is reflected in VEGF staining and quantification (Fig. 6D, E). Semiquantification of staining images showed a significant increase in VEGF staining in groups treated with both hPSCs and NELL-1 as compared to the groups with each treatment

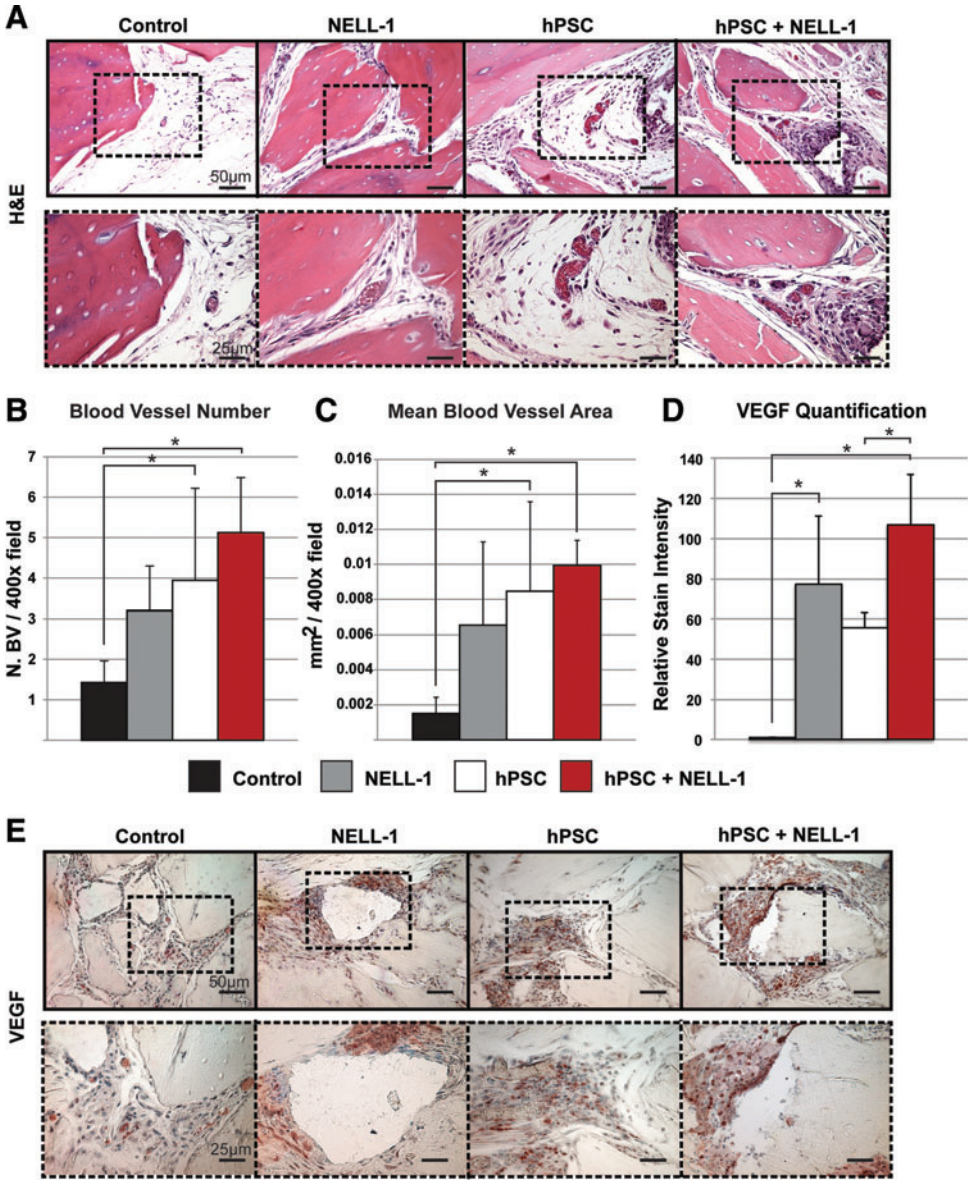

FIG. 6. NELL-1 enhances hPSC-mediated vascularization *in vivo*. H&E staining and VEGF immunohistochemistry were performed on the four previously mentioned experimental groups (DBX, DBX + NELL-1, DBX + hPSC, and DBX + hPSC + NELL-1). Histomorphometric semiquantitative analysis of respective 200× images followed using the Adobe Photoshop magic wand tool. **(A)** Representative H&E images. **(B)** Blood vessel number, based on $n = 10$ H&E images per group. **(C)** Mean blood vessel area, based on $n = 10$ H&E images per group. **(D)** VEGF stain quantification, based on $n = 7$ images per group at a tolerance of 30. **(E)** Representative image of VEGF immunohistochemistry. $^*p < 0.05$. Color images available online at www.liebertpub.com/tea

alone, consistent with our previous *in vitro* observations (see again Fig. 1J). These studies demonstrated the ability of NELL-1 to enhance hPSC-mediated vascularization.

Discussion

In summary, PSCs consist of two distinct cell populations known to exhibit characteristic MSC properties, and to share similar proliferation and bone-forming potential.[19] These include pericytes, which surround capillaries and microvessels, and adventitial cells, found in the tunica adventitia of large arteries and veins. As mentioned, PSCs can be isolated based on their differential expression of CD34 and CD146. In the present study, we expanded upon our original findings to explore the translational potential of PSCs as a population of pericytes and adventitial cells by examining both their osteogenic and vasculogenic properties. We demonstrated that PSCs undergo both *in vitro* and *in vivo* osteogenic differentiation, and that treatment with the craniosynostosis-associated osteoinductive protein, NELL-1, significantly augmented hPSC-mediated bone formation and vascularization.

hPSCs offer many advantages over conventional stem cell sources. PSCs are an abundant and purified osteoprogenitor cell population, and can be used immediately after sorting, bypassing culture expansion. This allows for direct implantation of cells from the FACS sorter to the patient, eliminating both the extra time and possible risks associated with *ex vivo* expansion. Further, hPSCs demonstrated a positive effect on vascularization, secreting significantly more VEGF than an equal number of SVF cells. hPSC treatment also resulted in significant increases in the blood vessel size and number. Interestingly, we found that implanted PSCs were often intimately associated with CD31+ endothelial cells, and in effect recapitulate their native perivascular origins. However, PSCs did not transdifferentiate into CD31+ endothelial cells, suggesting that their provasculogenic effect was primarily a supportive/trophic one. In summary, these

results suggest that hPSC-mediated vascularization holds potential in treating defects with poor blood flow, such as diabetic wounds and chronic bone defects.[34,35]

On the other hand, NELL-1 has a promising role in future bone regeneration therapies, owing to its osteoinductive and vasculogenic properties. A detailed review of NELL-1 signaling and its known effects can be found in a recent review article.[36] NELL-1 was first identified as osteoinductive via its overexpression in cranial sutures.[37] Studies involving over- and under-expression of NELL-1 in mice have yielded craniosynostotic and craniodysplastic defects, respectively.[38,39] Significant steps have already been made toward the use of recombinant NELL-1 for bone tissue engineering purposes. For example, prior studies in the rat intertransverse lumbar spine fusion[29] and sheep intrabody lumbar spine fusion[40] have shown a significant efficacy in the rate of fusion and degree of bone formation. Although NELL-1 is still in its clinical infancy and a human study has yet to be performed, its success in multiple small- and large-animal models suggests its promise as a candidate growth factor for future regenerative efforts.[19,29,32,40–42,*] In fact, unlike the commonly used BMPs, NELL-1 is highly specific to the osteochondral lineage and does not carry with it the undesirable pleiotropic effects observed with BMP-2.[19,36] For example, BMP-2 has been observed to induce a significant adipogenic response in various models, whereas NELL-1-treatment represses adipogenesis.[19,28,*] In the current study we directly compared the effect so BMP-2 and NELL-1 in PSC-mediated ectopic bone formation. Significantly, different qualities in bone regenerate were found: while BMP-2 induced a higher density of bone, this was also intermixed with lipid accumulation. NELL-1's specificity to bone was confirmed in previous studies comparing the nonskeletal abnormalities observed in BMP-2-deficient mice to the restricted skeletal defects present in NELL-1-deficient mice.[36,37,39,43] From a bone tissue engineering standpoint, osteogenic specificity is essential for reducing the potential for adverse clinical effects of a differentiation factor.[36,44] This is a significant concern, as the dose of BMP-2 required for successful osteogenesis in humans is associated with life-threatening cervical swelling, severe inflammation, increased adipogenesis, osseous overgrowth, and other complications.[36,45–48]

In addition, NELL-1 has significant effects on vascularization.[24] NELL-1's essential role in vascularization was confirmed with the observation that NELL-1-deficient embryos show reduced vasculogenesis during mid-gestation.[24] NELL-1's proangiogenic effect appears to be related to VEGF expression and function. Previous *in vitro* studies have demonstrated an increase in VEGF expression among human pericytes grown in a NELL-1-supplemented osteogenic medium.[24] Here, we demonstrate that the combined population of hPSCs treated with NELL-1 also showed significantly enhanced VEGF expression *in vivo*. Interestingly, VEGF shares additional similarities with NELL-1 and also participates in bone formation. Just as with NELL-1, for example, osteoblasts also secrete and respond to VEGF,[20] suggesting a role for VEGF in regulating the migration and differentiation of osteoblasts.[20,49,50] Little is known, however, about the degree to which NELL-1's provasculogenic effects are mediated by VEGF signaling.

In summary, the combination hPSC + NELL-1 product holds promise as a future cell- and growth-factor-based therapeutic. PSCs are easily harvestable by FACS and represent a ready-to-use purified osteoprogenitor cell population. Meanwhile, NELL-1 selectively induces osteogenic differentiation and enhances vascularization. Future studies will aim to further develop the translational potential of the hPSC + NELL-1 combination product by extending these findings to the skeletal defect-healing models for bone regeneration.

*Yuan, W. *et al.*, Assessment of high doses of BMP-2 and NELL-1 in an athymic rat posterolateral spine fusion model. J Orth Surg [In submission].

Acknowledgments

This work was supported by the CIRM Early Translational II Research Award TR2-01821, NIH/NIDCR (grants R21 DE0177711 and RO1 DE01607), UC Discovery Grant 07-10677, T32 training fellowship to A.W.J. (5T32DE007296-14), and CIRM Training Grant Research Fellowship to M.C. and J.N.Z. (TG-01169).

Disclosure Statement

Drs. X.Z., K.T., and C.S. are inventors of Nell-1-related patents and K.T., B.P., and C.S. are inventors of perivascular stem cell-related patents filed from UCLA. Drs. X.Z, K.T, and C.S. are founders of Bone Biologics, Inc., which sublicenses Nell-1 patents from the UC Regents, and Drs. K.T., and C.S. are founders of Scarless Laboratories, Inc., which sublicenses perivascular stem cell-related patents from the UC Regents. Dr. Chia Soo is also an officer of Scarless Laboratories, Inc.

References

1. Giannoudis, P.V., Dinopoulos, H., and Tsiridis, E. Bone substitutes: an update. Injury **36 Suppl 3,** S20, 2005.
2. Laurencin, C.T., Ambrosio, A.M., Borden, M.D., and Cooper, J.A., Jr. Tissue engineering: orthopedic applications. Annu Rev Biomed Eng **1,** 19, 1999.
3. Laurie, S.W., Kaban, L.B., Mulliken, J.B., and Murray, J.E. Donor-site morbidity after harvesting rib and iliac bone. Plast Reconstr Surg **73,** 933, 1984.
4. Frodel, J.L., Jr., Marentette, L.J., Quatela, V.C., and Weinstein, G.S. Calvarial bone graft harvest. Techniques, considerations, and morbidity. Arch Otolaryngol Head Neck Surg **119,** 17, 1993.
5. Cancedda, R., Mastrogiacomo, M., Bianchi, G., Derubeis, A., Muraglia, A., and Quarto, R. Bone marrow stromal cells and their use in regenerating bone. Novartis Found Symp **249,** 133; discussion 143, 170, 239, 2003.
6. Derubeis, A.R., and Cancedda, R. Bone marrow stromal cells (BMSCs) in bone engineering: limitations and recent advances. Ann Biomed Eng **32,** 160, 2004.
7. Zuk, P.A., Zhu, M., Ashjian, P., De Ugarte, D.A., Huang, J.I., Mizuno, H., Alfonso, Z.C., Fraser, J.K., Benhaim, P., and Hedrick, M.H. Human adipose tissue is a source of multipotent stem cells. Mol Biol Cell **13,** 4279, 2002.
8. Moerman, E.J., Teng, K., Lipschitz, D.A., and Lecka-Czernik, B. Aging activates adipogenic and suppresses osteogenic programs in mesenchymal marrow stroma/stem cells: the role of PPAR-gamma2 transcription factor and TGF-beta/BMP signaling pathways. Aging cell **3,** 379, 2004.
9. Giannoudis, P., Tzioupis, C., Almalki, T., and Buckley, R. Fracture healing in osteoporotic fractures: is it really dif-

ferent? A basic science perspective. Injury **38 Suppl 1,** S90, 2007.
10. Dahl, J.A., Duggal, S., Coulston, N., Millar, D., Melki, J., Shahdadfar, A., Brinchmann, J.E., and Collas, P. Genetic and epigenetic instability of human bone marrow mesenchymal stem cells expanded in autologous serum or fetal bovine serum. Int J Dev Biol **52,** 1033, 2008.
11. Cheung, W.K., Working, D.M., Galuppo, L.D., and Leach, J.K. Osteogenic comparison of expanded and uncultured adipose stromal cells. Cytotherapy **12,** 554, 2010.
12. Paredes, B., Santana, A., Arribas, M.I., Vicente-Salar, N., de Aza, P.N., Roche, E., Such, J., and Reig, J.A. Phenotypic differences during the osteogenic differentiation of single cell-derived clones isolated from human lipoaspirates. J Tissue Eng Regen Med **5,** 589, 2011.
13. Rajashekhar, G., Traktuev, D.O., Roell, W.C., Johnstone, B.H., Merfeld-Clauss, S., Van Natta, B., Rosen, E.D., March, K.L., and Clauss, M. IFATS collection: adipose stromal cell differentiation is reduced by endothelial cell contact and paracrine communication: role of canonical Wnt signaling. Stem Cells **26,** 2674, 2008.
14. Meury, T., Verrier, S., and Alini, M. Human endothelial cells inhibit BMSC differentiation into mature osteoblasts *in vitro* by interfering with osterix expression. J Cell Biochem **98,** 992, 2006.
15. Crisan, M., Yap, S., Casteilla, L., Chen, C.W., Corselli, M., Park, T.S., Andriolo, G., Sun, B., Zheng, B., Zhang, L., Norotte, C., Teng, P.N., Traas, J., Schugar, R., Deasy, B.M., Badylak, S., Buhring, H.J., Giacobino, J.P., Lazzari, L., Huard, J., and Peault, B. A perivascular origin for mesenchymal stem cells in multiple human organs. Cell Stem Cell **3,** 301, 2008.
16. Crisan, M., Corselli, M., Chen, C.W., and Peault, B. Multilineage stem cells in the adult: a perivascular legacy? Organogenesis **7,** 101, 2011.
17. Crisan, M., Chen, C.W., Corselli, M., Andriolo, G., Lazzari, L., and Peault, B. Perivascular multipotent progenitor cells in human organs. Ann N Y Acad Sci **1176,** 118, 2009.
18. Corselli, M., Chen, C.W., Sun, B., Yap, S., Rubin, J.P., and Peault, B. The tunica adventitia of human arteries and veins as a source of mesenchymal stem cells. Stem Cells Dev **21,** 1299, 2011.
19. James, A.W., Zara, J.N., Zhang, X., Askarinam, A., Goyal, R., Chiang, M., Yuan, W., Chang, L., Corselli, M., Shen, J., Pang, S., Stoker, D., Ting, K., Peault, B., and Soo, C. Perivascular stem cells: a prospectively purified mesenchymal stem cell population for bone tissue engineering. Stem Cells Transl Med **1,** 510, 2012.
20. Hsiong, S.X., and Mooney, D.J. Regeneration of vascularized bone. Periodontol 2000 **41,** 109, 2006.
21. Carmeliet, P., and Jain, R.K. Angiogenesis in cancer and other diseases. Nature **407,** 249, 2000.
22. Schor, A.M., Allen, T.D., Canfield, A.E., Sloan, P., and Schor, S.L. Pericytes derived from the retinal microvasculature undergo calcification *in vitro*. J Cell Sci **97 (Pt 3),** 449, 1990.
23. Canfield, A.E., Doherty, M.J., Wood, A.C., Farrington, C., Ashton, B., Begum, N., Harvey, B., Poole, A., Grant, M.E., and Boot-Handford, R.P. Role of pericytes in vascular calcification: a review. Z Kardiol **89 Suppl 2,** 20, 2000.
24. Zhang, X., Peault, B., Chen, W., Li, W., Corselli, M., James, A.W., Lee, M., Siu, R.K., Shen, P., Zheng, Z., Shen, J., Kwak, J., Zara, J.N., Chen, F., Zhang, H., Yin, Z., Wu, B., Ting, K., and Soo, C. The Nell-1 growth factor stimulates bone formation by purified human perivascular cells. Tissue Eng Part A **17,** 2497, 2011.
25. Chen, C.W., Montelatici, E., Crisan, M., Corselli, M., Huard, J., Lazzari, L., and Peault, B. Perivascular multi-lineage progenitor cells in human organs: regenerative units, cytokine sources or both? Cytokine Growth Factor Rev **20,** 429, 2009.
26. Levi, B., James, A.W., Nelson, E.R., Vistnes, D., Wu, B., Lee, M., Gupta, A., and Longaker, M.T. Human adipose derived stromal cells heal critical size mouse calvarial defects. PLoS One **5,** e11177, 2010.
27. James, A.W., Levi, B., Nelson, E.R., Peng, M., Commons, G.W., Lee, M., Wu, B., and Longaker, M.T. Deleterious effects of freezing on osteogenic differentiation of human adipose-derived stromal cells *in vitro* and *in vivo*. Stem Cells Dev **20,** 427, 2011.
28. James, A.W., Pan, A., Chiang, M., Zara, J.N., Zhang, X., Ting, K., and Soo, C. A new function of Nell-1 protein in repressing adipogenic differentiation. Biochem Biophys Res Commun **411,** 126, 2011.
29. Li, W., Lee, M., Whang, J., Siu, R.K., Zhang, X., Liu, C., Wu, B.M., Wang, J.C., Ting, K., and Soo, C. Delivery of lyophilized Nell-1 in a rat spinal fusion model. Tissue Eng Part A **16,** 2861, 2010.
30. James, A.W., Zara, J.N., Corselli, M., Chiang, M., Yuan, W., Nguyen, V., Askarinam, A., Goyal, R., Siu, R.K., Scott, V., Lee, M., Ting, K., Péault, B., and Soo, C. Use of human perivascular stem cells for bone regeneration. J Vis Exp **63,** e2952, 2012.
31. James, A.W., Theologis, A.A., Brugmann, S.A., Xu, Y., Carre, A.L., Leucht, P., Hamilton, K., Korach, K.S., and Longaker, M.T. Estrogen/estrogen receptor alpha signaling in mouse posterofrontal cranial suture fusion. PLoS One **4,** e7120, 2009.
32. Aghaloo, T., Jiang, X., Soo, C., Zhang, Z., Zhang, X., Hu, J., Pan, H., Hsu, T., Wu, B., and Ting, K. A study of the role of nell-1 gene modified goat bone marrow stromal cells in promoting new bone formation. Mol Ther **15,** 1872, 2007.
33. Zarrinkalam, M.R., Mulaibrahimovic, A., Atkins, G.J., and Moore, R.J. Changes in osteocyte density correspond with changes in osteoblast and osteoclast activity in an osteoporotic sheep model. Osteoporos Int **23,** 1329, 2012.
34. Bauer, S.M., Bauer, R.J., and Velazquez, O.C. Angiogenesis, vasculogenesis, and induction of healing in chronic wounds. Vasc Endovasc Surg **39,** 293, 2005.
35. Kanczler, J.M., and Oreffo, R.O. Osteogenesis and angiogenesis: the potential for engineering bone. Eur Cell Mater **15,** 100, 2008.
36. Zhang, X., Zara, J., Siu, R.K., Ting, K., and Soo, C. The role of NELL-1, a growth factor associated with craniosynostosis, in promoting bone regeneration. J Dent Res **89,** 865, 2010.
37. Ting, K., Vastardis, H., Mulliken, J.B., Soo, C., Tieu, A., Do, H., Kwong, E., Bertolami, C.N., Kawamoto, H., Kuroda, S., and Longaker, M.T. Human NELL-1 expressed in unilateral coronal synostosis. J Bone Miner Res **14,** 80, 1999.
38. Zhang, X., Ting, K., Pathmanathan, D., Ko, T., Chen, W., Chen, F., Lee, H., James, A.W., Siu, R.K., Shen, J., Culiat, C.T., and Soo, C. Calvarial cleidocraniodysplasia-like defects with ENU-induced Nell-1 deficiency. J Craniofac Surg **23,** 61, 2012.
39. Zhang, X., Kuroda, S., Carpenter, D., Nishimura, I., Soo, C., Moats, R., Iida, K., Wisner, E., Hu, F.Y., Miao, S., Beanes, S., Dang, C., Vastardis, H., Longaker, M., Tanizawa, K., Kanayama, N., Saito, N., and Ting, K. Craniosynostosis in transgenic mice overexpressing Nell-1. J Clin Invest **110,** 861, 2002.

40. Siu, R.K., Lu, S.S., Li, W., Whang, J., McNeill, G., Zhang, X., Wu, B.M., Turner, A.S., Seim, H.B., Hoang, P., Wang, J.C., Gertzman, A.A., Ting, K., and Soo, C. Nell-1 protein promotes bone formation in a sheep spinal fusion model. Tissue Eng Part A **17,** 1123, 2011.
41. Li, W., Zara, J.N., Siu, R.K., Lee, M., Aghaloo, T., Zhang, X., Wu, B.M., Gertzman, A.A., Ting, K., and Soo, C. Nell-1 enhances bone regeneration in a rat critical-sized femoral segmental defect model. Plast Reconstr Surg **127,** 580, 2011.
42. Lu, S.S., Zhang, X., Soo, C., Hsu, T., Napoli, A., Aghaloo, T., Wu, B.M., Tsou, P., Ting, K., and Wang, J.C. The osteoinductive properties of Nell-1 in a rat spinal fusion model. Spine J **7,** 50, 2007.
43. Zhang, H., and Bradley, A. Mice deficient for BMP2 are nonviable and have defects in amnion/chorion and cardiac development. Development **122,** 2977, 1996.
44. Walker, D.H., and Wright, N.M. Bone morphogenetic proteins and spinal fusion. Neurosurg Focus **13,** e3, 2002.
45. Carragee, E.J., Hurwitz, E.L., and Weiner, B.K. A critical review of recombinant human bone morphogenetic protein-2 trials in spinal surgery: emerging safety concerns and lessons learned. Spine J **11,** 471, 2011.
46. Riew, K.D., Wright, N.M., Cheng, S., Avioli, L.V., and Lou, J. Induction of bone formation using a recombinant adenoviral vector carrying the human BMP-2 gene in a rabbit spinal fusion model. Calcif Tissue Int **63,** 357, 1998.
47. Poynton, A.R., and Lane, J.M. Safety profile for the clinical use of bone morphogenetic proteins in the spine. Spine (Phila Pa 1976) **27,** S40, 2002.
48. Haid, R.W., Jr., Branch, C.L., Jr., Alexander, J.T., and Burkus, J.K. Posterior lumbar interbody fusion using recombinant human bone morphogenetic protein type 2 with cylindrical interbody cages. Spine J **4,** 527; discussion 538, 2004.
49. Mayr-Wohlfart, U., Waltenberger, J., Hausser, H., Kessler, S., Gunther, K.P., Dehio, C., Puhl, W., and Brenner, R.E. Vascular endothelial growth factor stimulates chemotactic migration of primary human osteoblasts. Bone **30,** 472, 2002.
50. Midy, V., and Plouet, J. Vasculotropin/vascular endothelial growth factor induces differentiation in cultured osteoblasts. Biochem Biophys Res Commun **199,** 380, 1994.

Address correspondence to:
Chia Soo, MD, FACS
Division of Plastic and Reconstructive Surgery
Departments of Surgery and Orthopaedic Surgery
David Geffen School of Medicine at UCLA
University of California, Los Angeles
675 Charles E Young Dr South, MRL 2641A
Los Angeles, CA 90095-1579

E-mail: bsoo@ucla.edu

Received: June 12, 2012
Accepted: January 16, 2013
Online Publication Date: April 3, 2013